

Performance of lithium-manganese oxide spinel electrodes in a lithium polymer electrolyte cell

W. J. Macklin*, R. J. Neat and R. J. Powell

Applied Electrochemistry Department, AEA Industrial Technology, Harwell Laboratory, Oxfordshire, OX11 0RA (UK)

(Received May 22, 1990, in revised form July 30, 1990)

Abstract

The cycling performance of a lithium-manganese oxide spinel (prepared from MnO_2 and Li_2CO_3) has been investigated as a function of preparation temperature in a lithium polymer electrolyte cell. Excellent reversibility and high rate performance have been observed from a spinel phase prepared at 450 °C and of general formula $\text{Li}_{1-x}\text{Mn}_{2-x}\text{O}_4$ ($0 \leq x \leq 1.33$, $0 \leq z \leq 0.33$). This phase has a characteristic cubic lattice parameter of $\sim 8.19 \text{ \AA}$ less than that found in the stoichiometric spinel material LiMn_2O_4 .

Introduction

Lithium insertion reactions with manganese oxides are of both scientific and technical interest. Manganese dioxide is now used worldwide as a solid cathode material for lithium primary batteries. During the last few years, however, remarkable progress has been made in the development of rechargeable Li/MnO_2 cells [1]. Reversible insertion of Li^+ ions has been reported in both spinel-type $\lambda\text{-MnO}_2$ [2] and spinel-type $\gamma\text{-MnO}_2$ [3] and in heat treated $\text{LiOH} \cdot \text{MnO}_2$ [4, 5]. Of particular interest is the system $\text{Li}_{1+x}\text{Mn}_2\text{O}_4$ in which the $[\text{Mn}_2\text{O}_4]$ framework possesses a 3D interstitial space via face-sharing octahedra and tetrahedra. This provides a conducting pathway for Li^+ ions which remains intact for both lithium insertion and extraction over the range $-1 < x < 1$ [4]. The cubic spinel structure ($Fd\bar{3}m$) is shown in Fig. 1. The mixed B-site valency results in good electronic conductivity [6], an essential property for a high rate, solid-state cathode material. Lithium insertion into LiMn_2O_4 induces a Jahn-Teller distortion which reduces the crystal symmetry from cubic in LiMn_2O_4 to tetragonal in $\text{Li}_{1+x}\text{Mn}_2\text{O}_4$, resulting in a two-phase electrode, which produces a desirable, flat, open-circuit voltage of $\sim 2.9 \text{ V}$, Fig. 2.

Although relatively high polarisation was reported in early $\text{Li}/\text{Li}_{1+x}\text{Mn}_2\text{O}_4$ cells and was attributed to low Li^+ ion mobility in the manganese spinel [4], both Sony [7, 8] and Moli Energy [9], have recently announced secondary lithium batteries based on a lithium-manganese oxide. In addition, a number

*Author to whom correspondence should be addressed

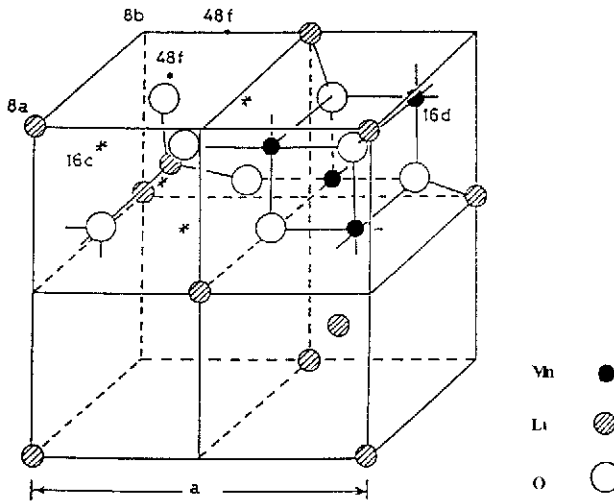


Fig 1 The spinel structure ($Fd\bar{3}m$)

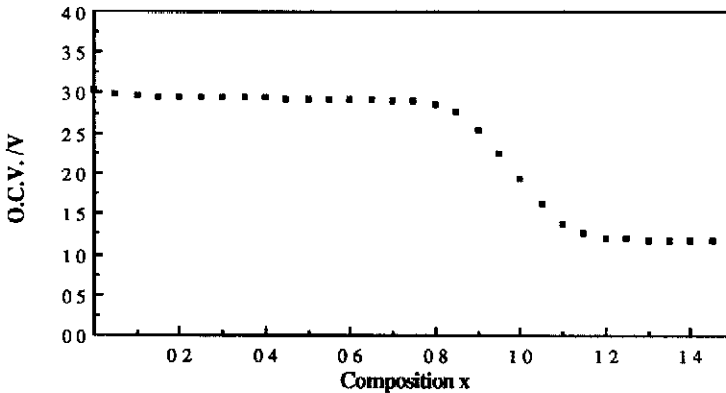


Fig 2 Open-circuit voltage of $\text{Li}_{1+x}\text{Mn}_2\text{O}_4$ vs composition x

of recent patent applications from leading battery manufacturers [10–12] suggest further commercial development in this area

The discovery of polymeric solid electrolytes based on complexes of poly(ethylene oxide) (PEO) and lithium salts (e.g., LiClO_4 , LiCF_3SO_3) by Armand and co-workers [13] has led to the development of high energy density lithium polymer batteries [14–16]. In previous work [17] we reported results on the rechargeability of MnO_2 in the lithium polymer cell and demonstrated the *in situ* conversion of MnO_2 to the spinel $\text{Li}_x\text{Mn}_2\text{O}_4$. The excellent reversibility of the resultant $\text{Li}_x\text{Mn}_2\text{O}_4$ has led us to investigate the performance of this material in a lithium polymer electrolyte cell and, in particular, to consider the effect of sample preparation conditions on performance

Experimental

Lithium–manganese oxide samples were prepared at four different sintering temperatures: 450 °C, 500 °C, 600 °C and 800 °C. Manganese dioxide (electrolytic) and Li_2CO_3 (Aldrich 99.999%) were thoroughly ground and then sintered in air in an alumina crucible for 16 h at the desired temperature. Repeated grinding and sintering followed until no change was observed in the X-ray diffraction pattern. These patterns were obtained using a Philips PW 1050 goniometer employing $\text{Cu K}\alpha$ radiation and incorporating pulse height discrimination and a curved graphite secondary monochromator. Data collection and processing over the range $4^\circ \leq 2\theta \leq 70^\circ$ was controlled by a PDP11/23 plus computer.

Composite cathodes containing lithium–manganese oxide sample, ketjenblack carbon, PEO (Union Carbide MW 4000000) and LiClO_4 (Aldrich) were prepared via doctor blade casting from the appropriate solvent slurry onto a nickel current collector [18]. The resulting cathodes had the composition 45 vol.% lithium–manganese oxide, 5 vol.% carbon and 50 vol.% PEO– LiClO_4 ($[\text{EO units}]/[\text{Li}] = 12$) with a capacity of $\sim 0.5 \text{ mA h cm}^{-2}$ based on a value of 151 mA h g^{-1} for LiMn_2O_4 , corresponding to the insertion of one lithium into LiMn_2O_4 and an energy density of $\sim 440 \text{ W h kg}^{-1}$. Sheets of the electrolyte PEO– LiClO_4 ($[\text{EO units}]/[\text{Li}] = 12$) were cast from acetonitrile solution onto silicone release paper. This electrolyte composition had been found previously to have the highest ionic conductivity at 120 °C. Solid-state cells incorporating a lithium foil anode (Lithco 150 μm) with an active area of 40 cm^2 were constructed in a dry room ($T = 20^\circ \text{C}$, dew point temperature -30°C) using a combination of heat and pressure. The cell configuration is shown in Fig. 3. The cells were packaged and placed in an oven at 120 °C for testing.

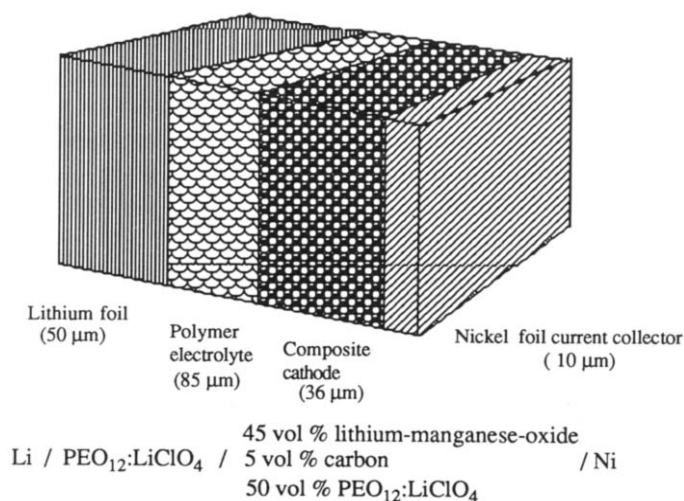


Fig. 3 The lithium polymer electrolyte cell configuration

The a.c. impedance measurements were carried out with a Solartron 1254 frequency response analyser over the frequency range 65 kHz–0.1 Hz in combination with a Solartron 1286 electrochemical interface. Cell cycling was performed on a computer-controlled charge/discharge rig at constant current between preset voltage limits.

Chemical analysis of lithium–manganese oxide samples was carried out by Inductively Coupled Plasma/Optical Emission Spectroscopy using an ARL 3560 Spectrometer.

Results and discussion

X-ray diffraction analysis indicated that the major phase in all four samples was a cubic spinel [19], Fig. 4(a)–(d). The measured lattice parameter of 8.245 Å for the 800 °C sample is in good agreement with that reported for the stoichiometric spinel LiMn_2O_4 [20]. In the samples prepared at lower temperatures a second manganese oxide phase, Mn_2O_3 (bixbyite) was detected; the proportion of which increased with decreasing sintering temperature. A detailed inspection of the X-ray diffraction patterns for the four different samples, Fig. 5, reveals several other important differences.

First, there is an observed decrease in the cubic lattice parameter, a , for the spinel phase with lower sintering temperatures, see Table 1. Lithium extraction from LiMn_2O_4 ultimately yields cubic Mn_2O_4 , commonly referred to as $\lambda\text{-MnO}_2$ [21], with a reported cubic lattice parameter of 8.029 Å [20]. Lithium-defect spinel phases $\text{Li}_{1-x}\text{Mn}_2\text{O}_4$, ($0 < x < 1$) have intermediate a values between 8.029 Å ($x = 1$) and 8.245 Å ($x = 0$) [22]. On this basis, the measured lattice parameter of ~ 8.19 Å for the 450 °C and 500 °C samples corresponds to a lithium-deficient spinel phase of approximate composition $\text{Li}_{0.7}\text{Mn}_2\text{O}_4$. However, chemical analysis of all four samples gave a lithium to manganese ratio of 1.01200, and since X-ray diffraction analysis suggests an absence of additional lithium-containing phases, the existence of $\text{Li}_{0.7}\text{Mn}_2\text{O}_4$ is unlikely. An alternative explanation involves the formation of a defect spinel phase in which manganese vacancies exist on the octahedral sites of the spinel structure. As the preparation temperature increases, the amount of the minority phase, Mn_2O_3 , is reduced, consistent with a decrease in the number of manganese vacancies, such that at 800 °C the composition approaches that of the stoichiometric spinel LiMn_2O_4 .

A recent neutron diffraction study [23] obtained data on the reaction product of a 1:1 mixture of Mn_2O_3 and Li_2CO_3 sintered at a range of different temperatures. The neutron diffraction patterns showed that the product was characterised by a spinel phase, $\text{Li}_{1+z}\text{Mn}_{2-z}\text{O}_4$ (where $0 \leq z \leq 1.33$ and $0 < z \leq 0.33$), Li_2MnO_3 , and a minor concentration of unreacted Mn_2O_3 . They reported cubic lattice parameters of 8.159 Å and 8.196 Å for samples prepared at 500 °C and 600 °C, respectively.

A second difference in the X-ray diffraction patterns is the increase in peak widths with decreasing temperature of preparation. In Table 1 the peak

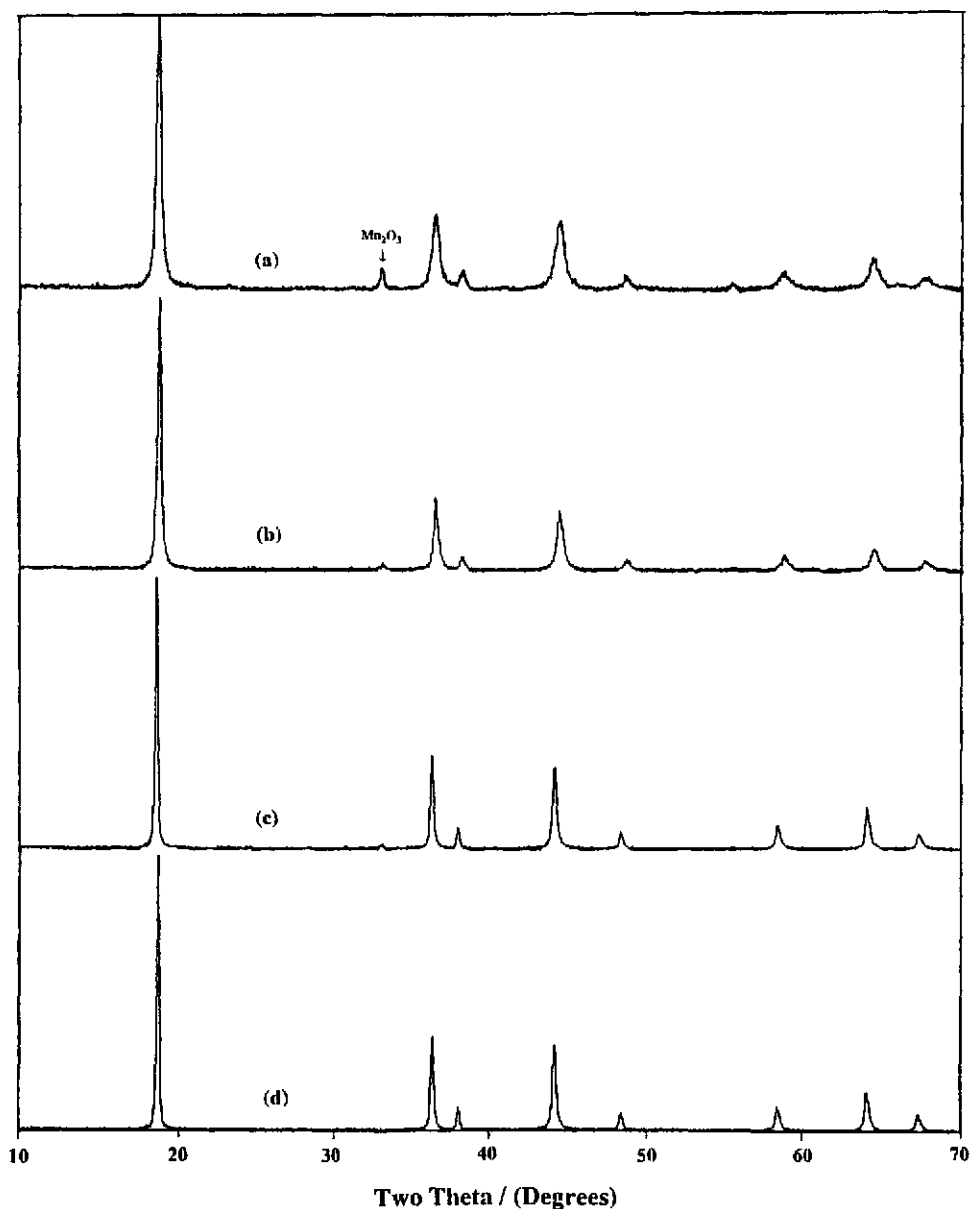


Fig 4 Powder X-ray diffraction patterns of the product of the reaction $\text{Li}_2\text{CO}_3 + \text{MnO}_2$ at (a) 450 °C, (b) 500 °C, (c) 600 °C, (d) 800 °C

width at half maximum height (FWHM) is given for the (311) reflection observed at $2\theta \sim 36^\circ$ for each of the lithium-manganese oxide samples. A similar trend in line broadening with temperature has previously been observed in both X-ray diffraction [10] and neutron diffraction [23] data on the

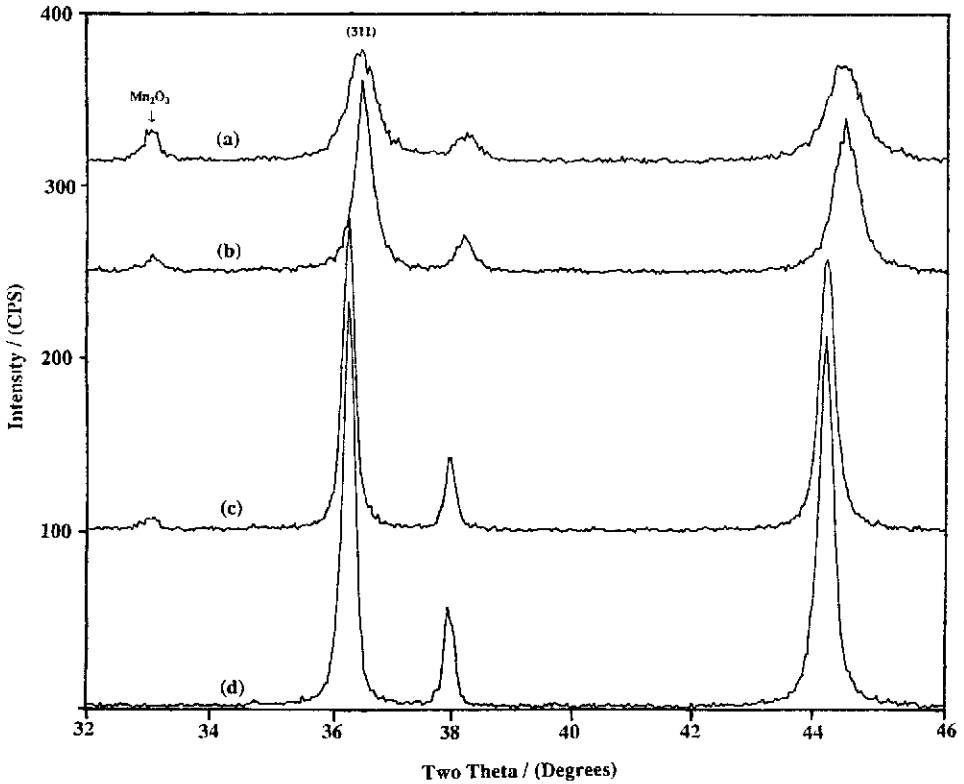


Fig 5 Detailed X-ray diffraction patterns of the product of the reaction $\text{Li}_2\text{CO}_3 + \text{MnO}_2$ at (a) 450 °C, (b) 500 °C, (c) 600 °C, (d) 800 °C, over the range $32^\circ \leq 2\theta \leq 46^\circ$

TABLE 1

Peak width at maximum height data

Temperature (°C)	Lattice parameter (Å)	FWHM (311) reflection ($^\circ 2\theta$)
450	8 190 (5)	0 53
500	8 193 (5)	0 30
600	8 231 (3)	0 24
800	8 245 (3)	0 22

formation of the spinel phase. One possible cause of the observed line broadening in the diffraction pattern is a scatter of interplanar spacing in the diffracting volume [24], usually described as strain. In this case we may attribute the observed strain to growth defects and inhomogeneities in the stoichiometry of the spinel phases generated at the lower sintering temperatures.

The a.c. impedance data obtained after 2 h at 120 °C, Fig. 6, indicate the very low overall impedance of the $\text{Li}/\text{PEO}_{12}\cdot\text{LiClO}_4/\text{lithium-manganese}$

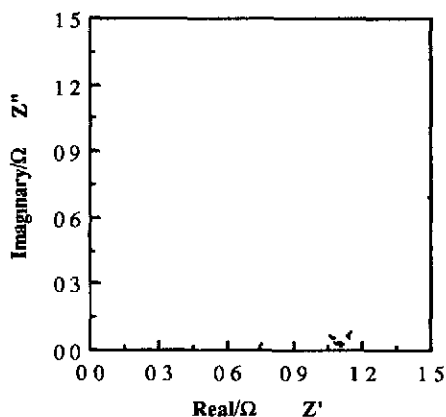


Fig 6 The a.c impedance plot of an $\text{Li/PEO}_{12} \text{LiClO}_4/\text{lithium-manganese oxide}$ cell

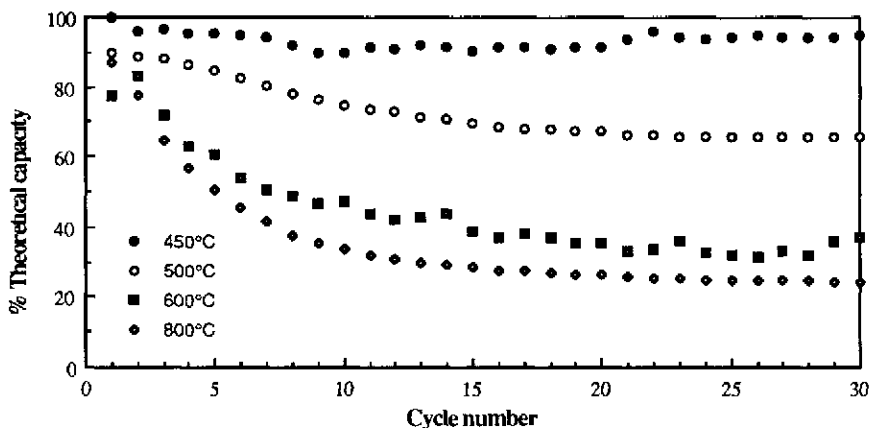


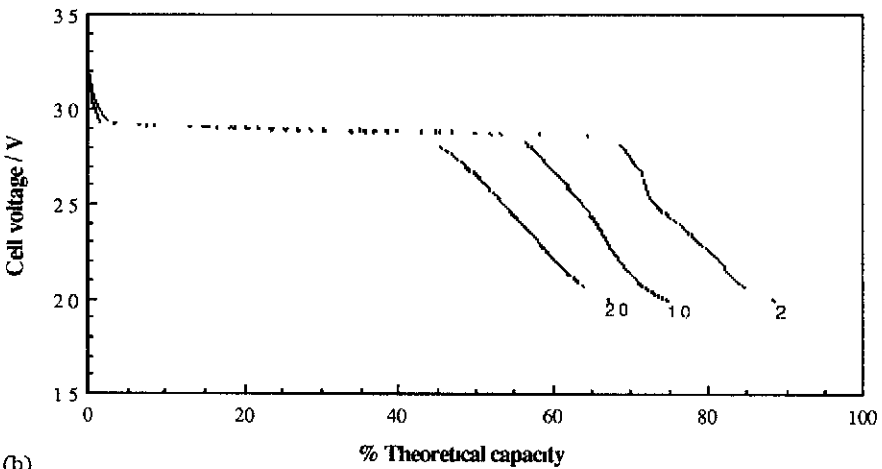
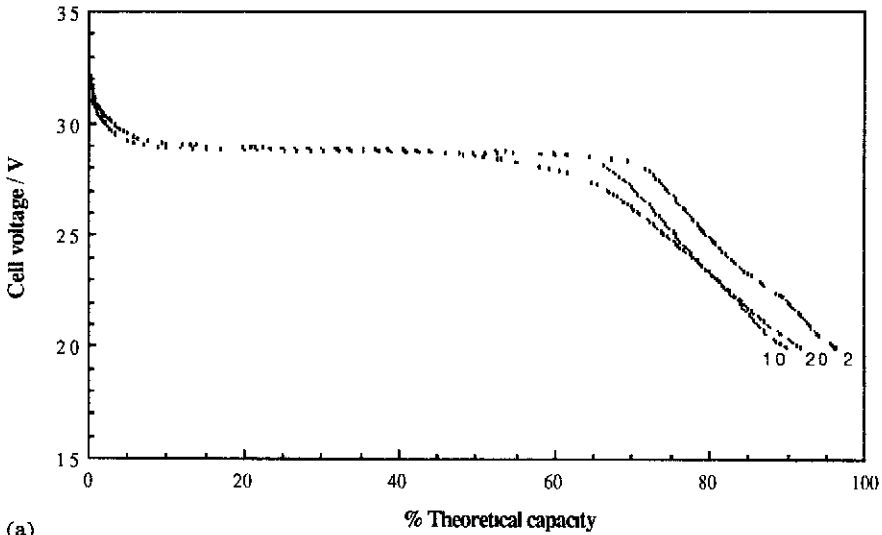
Fig 7 The percentage theoretical capacity obtained vs cycle number for cells containing lithium-manganese oxide samples prepared at different temperatures

oxide cells. The low series resistance reflects both the high conductivity of the electrolyte ($\sim 10^{-3} \text{ S cm}^{-1}$) and the adequate electronic conductivity of the composite cathode. There was no observable difference between the impedance plots of the cells containing the different LiMn_2O_4 samples.

Cells containing the four different lithium-manganese oxide samples were cycled at the $C/10$ rate between voltage limits of 3.25 and 2.0 V. The percentage of theoretical capacity obtained is plotted against cycle number for the first thirty cycles in Fig 7. We observe a large capacity decline from the 600 °C and 800 °C samples within the first ten cycles, with further cycling at only $\sim 30\%$ theoretical capacity. While the 500 °C sample cycled reversibly at 65% theoretical capacity after fifteen cycles, the 450 °C sample demonstrated far superior capacity retention. Figure 8 shows the 2nd, 10th, and 20th discharge curves for each type of cell. On analysis of the voltage-time

data, it is clear that the capacity decline is associated with a shortening of the plateau at ~ 2.9 V, corresponding to the two-phase region of cubic and tetragonal forms of $\text{Li}_{1+x}\text{Mn}_2\text{O}_4$. In the case of the 450°C material, although there is only a minor loss of capacity, a structural change is indicated by the loss of the well-defined end to the plateau with increasing cycle number.

The cycling performance reported above indicates that lithium ion insertion reversibility is clearly related to the temperature of preparation of the spinel material. The significantly greater reversibility of the 450°C sample may be associated with a higher Li^+ ion mobility in the defect $\text{Li}_x\text{Mn}_{2-z}\text{O}_4$ spinel than that found in the stoichiometric LiMn_2O_4 phase, and resembles that



(b)
Fig 8

previously observed from the spinel phase generated *in situ* from MnO_2 [17]. In the case of the latter material the extensive line broadening in the X-ray diffraction pattern prevented the determination of an accurate cubic lattice parameter and, hence, the stoichiometry. Analogous behaviour has recently been reported for CuO [25], where the thermal pretreatment of CuO samples influenced their electrochemical activity as a cathode material in a lithium cell. The defects observed in the microstructure of the CuO samples annealed at lower temperatures (up to 400°C) were considered favourable for the diffusion of Li ions into the CuO lattice, and resulted in significantly better cell performance.

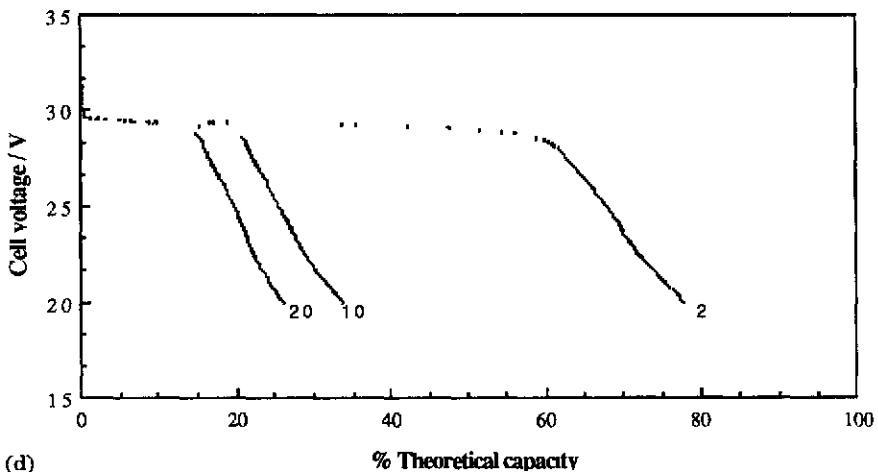
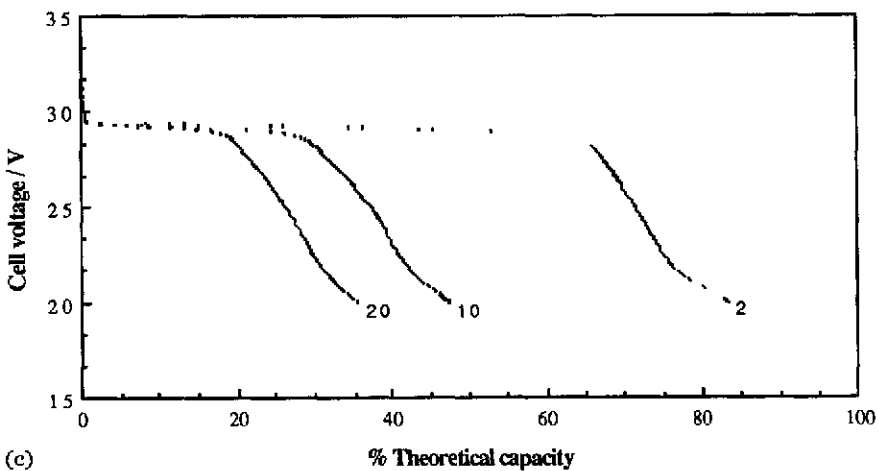


Fig 8 The 2nd, 10th, and 20th discharge curves for a lithium polymer electrolyte cell containing a lithium-manganese oxide sample prepared at (a) 450°C , (b) 500°C , (c) 600°C , (d) 800°C

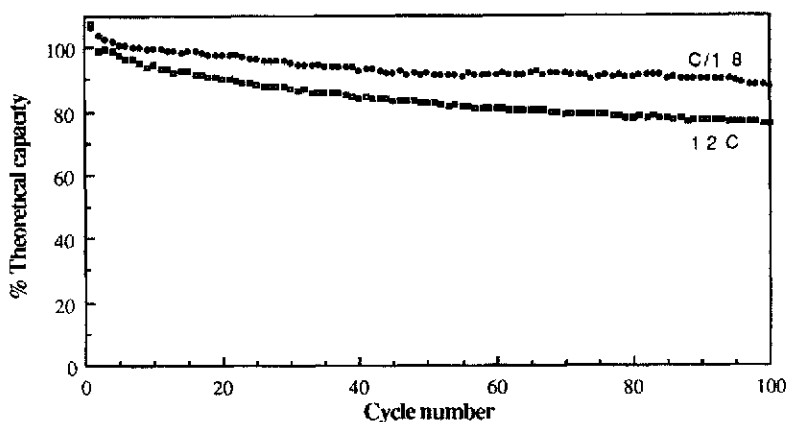


Fig 9 Cycling data at 1.2 C and C/1.8 rates for a lithium polymer electrolyte cell containing lithium-manganese oxide prepared at 450 °C

The excellent cyclability of the 450 °C material in a lithium polymer electrolyte cell has also been demonstrated at high rates (up to 1.2 C), Fig 9. This would be advantageous in traction applications, where the ability of a battery to sustain fast (0.5–1 h) charging would help solve the problem of the limited range in electric vehicles, and make the need for battery interchange superfluous.

Conclusions

The spinel phase resulting from the reaction of MnO_2 and Li_2CO_3 at temperatures of ~ 450 °C exhibits excellent reversibility and good rate performance in the lithium polymer electrolyte cell. Although the theoretical specific energy density of $\text{Li}_{1+x}\text{Mn}_{2-x}\text{O}_4$, $0 < x < 1$ (~ 440 W h kg^{-1}), is less than that of some other cathode materials currently under investigation for lithium secondary batteries such as V_6O_{13} (~ 880 W h kg^{-1}), it may prove to be a superior cathode material both in terms of cost and for extended cycling performance.

Acknowledgements

The authors thank F. Cullen for the X-ray diffraction analysis and D. Brown for the chemical analysis.

References

- 1 J. Desilvestro and O. Haas, *J. Electrochem. Soc.*, 137 (1990) 5C.

- 2 J. C. Hunter and F. B. Tadron, *Proc. Electrochem. Soc.*, 85-4 (1985) 444.
- 3 M. M. Thackeray, A. De Kock, L. A. De Picciotto and G. Pistoia, *J. Power Sources*, 26 (1989) 355.
- 4 M. M. Thackeray, A. De Kock, L. A. De Picciotto, P. J. Johnson, V. A. Nicholas and K. T. Andendorff, *J. Power Sources*, 21 (1987) 1.
- 5 T. Nohma, T. Saito, N. Furukawa and H. Ikeda, *J. Power Sources*, 26 (1989) 389.
- 6 M. M. Thackeray, W. I. F. David, P. G. Bruce and J. B. Goodenough, *Mater. Res. Bull.*, 18 (1983) 461.
- 7 *Battery and EV Technol.*, 12 (7) (1988) 2.
- 8 *Sony's Lithium Manganese Rechargeable Battery (AA size)*, JEC Press Inc., Feb. 1988.
- 9 *Moli Energy's New Product Data Sheet*, JEC Battery Newsletter No. 6 (Nov.-Dec.), 1988, p. 15.
- 10 J. Nagaura, M. Yokokawa and T. Hashimoto, *U.K. Patent Applic. GB 2 196 785* (1988).
- 11 N. Furukawa, T. Saito and T. Nohma, *Eur. Patent Applic. 0 265 950* (1987).
- 12 N. Furukawa, T. Ohsumigaoka and T. Nohma, *Eur. Patent Applic. 0 279 235* (1988).
- 13 M. B. Armand, J. B. Chabagno and M. J. Duclot, in P. Vashishta, J. N. Mundy and G. K. Shenoy (eds.), *Fast Ion Transport in Solids*, North Holland, New York, 1979, p. 131.
- 14 M. B. Armand, *Solid State Ionics*, 9&10 (1983) 745.
- 15 A. Hooper and B. C. Tofield, *J. Power Sources*, 11 (1984) 33.
- 16 M. Gauthier, D. Fateux, G. Vassort, A. Belanger, M. Duval, P. Ricoux, J. Chabagno, D. Muller, P. Rigaud, M. Armand and D. Deroo, *J. Electrochem. Soc.*, 132 (1985) 1333.
- 17 R. J. Neat, W. J. Macklin and R. J. Powell, in B. Scrosati (ed.), *Second Int. Symp. Polymer Electrolytes*, Elsevier, Amsterdam/New York, 1990, p. 421.
- 18 A. Hooper and J. M. North, *Solid State Ionics*, 9&10 (1983) 1161.
- 19 Joint Committee on Powder Diffraction Standards, *JCPDS 35-0782*.
- 20 A. Masbah, A. Verbaux and M. Tournoux, *Mater. Res. Bull.*, 18 (1983) 1375.
- 21 J. C. Hunter, *J. Solid State Chem.*, 39 (1981) 142.
- 22 W. I. F. David, M. M. Thackeray, L. A. De Picciotti and J. B. Goodenough, *J. Solid State Chem.*, 67 (1987) 316.
- 23 M. Il. Rossouw, A. DeKock, L. A. De Picciotto, M. M. Thackeray, W. I. F. David and R. M. Ebberson, *Mater. Res. Bull.*, 25 (1990) 173.
- 24 H. P. Klug and L. E. Alexander, *X-ray Diffraction Procedures for Polycrystalline and Amorphous Materials*, Wiley, New York, 1970.
- 25 P. Podhajecky, Z. Zabransky, P. Novak, Z. Dobiasova, R. Cerny and V. Valvoda, *Electrochim. Acta*, 35 (1990) 245.